



# Using Filters to Estimate Regional Lung Deposition with Pressurized Metered Dose Inhalers

Scott Tavernini<sup>1</sup> · Dino J. Farina<sup>2</sup> · Andrew R. Martin<sup>1</sup> · Warren H. Finlay<sup>1</sup>

Received: 24 August 2022 / Accepted: 15 October 2022 / Published online: 8 November 2022  
© The Author(s), under exclusive licence to Springer Science+Business Media, LLC, part of Springer Nature 2022

## Abstract

**Purpose** To evaluate the suitability of a recently proposed apparatus that uses filters to directly fractionate the *in vitro* lung dose into regional deposition estimates for use with pressurized metered dose inhaler (pMDI) devices as a less resource intensive alternative to cascade impaction.

**Methods** Using three commercially available pMDI devices (Asmanex HFA, Ventolin HFA, QVAR), regional deposition estimates were measured directly using the filter-based apparatus (FBA). Regional deposition estimates were also generated for the same inhalers by performing cascade impaction measurements and inputting the results to an *in silico* regional deposition model. Regional deposition for each inhaler was evaluated at an inhalation flow rate of 30 and 60 L/min.

**Results** Total recovery of active pharmaceutical ingredient and extrathoracic deposition was independent of method used. The regional deposition estimates provided by each method were similar and captured the same trends.

**Conclusions** The direct measurement of estimated regional deposition is possible when using the FBA. This method is far less resource intensive than existing methods and so may be useful both for comparison of generic alternatives and the development of innovative products.

## Introduction

*In vitro* quantification and qualification of orally inhaled drug products is extensively used as a measure of quality assurance and quality control (QA/QC); the same methods are also used to inform new product development and demonstrate equivalence of generic alternatives to previously approved products. When using these methods in the latter two capacities, researchers must understand their limitations and implement enhancements to improve the correlation of *in vitro* results to expected *in vivo* outcomes.

For QA/QC purposes, delivered dose uniformity (measured with a dose uniformity sampling apparatus) and the aerodynamic particle size distribution (APSD, measured by cascade impaction) can be determined using

the methods described in the appropriate pharmacopeia documents [1, 2]. Delivered dose uniformity provides a measure of the entire delivered dose of active pharmaceutical ingredient (API) while the APSD relates to the anticipated *in vivo* deposition profile. However, the simplifications that make cascade impactor methods standardized, repeatable, and simple preclude meaningful estimation of the deposition site of the emitted API. In particular, the use of a highly simplified induction port results in coarse particles being characterized by the impactor. This problem is partially addressed by the determination of the fine particle fraction (FPF), which is generally defined as the fraction of the delivered dose with an aerodynamic diameter less than 5  $\mu\text{m}$ . While this size is explicitly defined by the European Pharmacopeia [1], the United States Pharmacopeia [2] allows the specific size to be defined by the individual product monograph; this combined with users making the convenient choice of using a specific impactor stage to define the FPF (thereby eliminating the need to interpolate between stages) results in FPF upper size limits ranging in the literature between 4.5 and 6.8  $\mu\text{m}$  [3]. Also referred to as the respirable dose, the FPF is sometimes considered to be commensurate with the lung dose, but the deposition site (extrathoracic vs. lung) of particles

✉ Andrew R. Martin  
andrew.martin@ualberta.ca

✉ Warren H. Finlay  
warren.finlay@ualberta.ca

<sup>1</sup> Department of Mechanical Engineering, University of Alberta, Edmonton, AB, Canada

<sup>2</sup> Proveris Scientific Corporation, Hudson, MA, USA

around the FPF limit will depend strongly on the kinetics of the inhaler and the inhalation maneuver of the patient. Finally, the FPF alone omits any measure of the width (or geometric standard deviation [GSD]) of the particle size distribution; two aerosol clouds could have an identical FPF yet significantly different widths, resulting in differing deposition patterns for the two aerosol clouds *in vivo* [3].

The first and simplest step in improving the pharmacopeial methods is to use an induction port that mimics extrathoracic deposition in the human population [3, 4] such as the Alberta Idealized Throat (AIT). When such an induction port is used, the dose depositing in the cascade impactor is representative of the expected lung dose and can be characterized by its mass median aerodynamic diameter (MMAD) and GSD, allowing further analysis using advanced *in silico* methods to predict regional deposition of this dose within the lung [5]. Others [6, 7] have proposed using impactors with fewer stages, called fast screening impactors (FSI), for abbreviated impactor measurements (AIM) to fractionate this *in vitro* lung dose directly into FPF and extra-fine particle fractions to reduce the resource burden associated with full resolution impactor measurements. These fractions cannot be directly associated with *in vivo* deposition in regions of the lungs since deposition site/proportions will depend on the inhalation profile generated by the patient. Further, this approach prohibits accurate estimation of regional lung deposition because the resolution of the distribution is lost.

An additional step in improving the pharmacopeial methods involves generating realistic inhalation patterns through the inhaler and extrathoracic model. This is most important for dry powder inhalers, where the inhalation provides the energy source for aerosolization and deagglomeration of the powder, but is also useful for testing delayed inhalation with pressurized metered dose inhalers (pMDIs) and soft mist inhalers (SMIs) [4] for which poor patient coordination could reduce device performance. Cascade impactors, however, must be operated at specified, fixed flow rates for which they are calibrated. Additional equipment (mixing inlet, makeup flow supply line with flow monitoring, and breath generator) can be incorporated into the cascade impactor apparatus to enable time varying inhalations to be performed through the inhaler while the cascade impactor remains under constant flow [8, 9]. This is a significantly more complicated experiment to conduct and also sets an upper limit on flow rate, imposed by the maximum flow rate for which the cascade impactor has been calibrated.

Recently, a new device has been proposed which uses a specially designed filter [10] to capture the tracheobronchial (TB) dose from the aerosol cloud penetrating an idealized extrathoracic geometry and leaves the remaining aerosol to be captured by an additional final filter. This device is

intended to alleviate the complexity and resource burden associated with cascade impactor measurements while providing reasonable *in vitro in vivo* correlation. Using a realistic induction port (i.e., the AIT) in conjunction with the TB filter apparatus and a final filter to capture the aerosol remaining after traversing the TB filter allows for simple and rapid determination of expected regional deposition. Since the AIT has been designed to remove the extrathoracic fraction, the aerosol leaving the AIT is representative of the lung dose. Then, by the same logic, since the TB Filter has been designed to remove the TB fraction of the lung dose, the aerosol leaving that apparatus represents the alveolar dose and can be collected on a filter capturing all remaining particles. This approach assumes there is no exhaled dose, a reasonable assumption for most single breath inhalers. Thus, the aerosol is physically fractionated into regional deposition estimates, and the mass of API on each collection surface simply needs to be determined using a suitable assay. The use of this method with DPIs has been demonstrated [11] but it has not yet been evaluated for use with pMDIs.

The present study examines the ability of this filter-based apparatus (FBA) to provide regional deposition estimates in agreement with an *in silico* model that uses the results of traditional cascade impactor measurements as input to generate regional lung deposition estimates for a selection of pMDI devices.

## Methods

Regional deposition estimates were obtained for three different commercially available pMDI devices: Asmanex HFA (Lot U019924, Merck & Co., Inc., Whitehouse Station, NJ, USA), QVAR (Lot GUL037A, Valeant Canada LP, Laval, Canada), and Ventolin HFA (Lot RX4E, GlaxoSmithKline Inc., Mississauga, Canada). Additional inhaler details are available in Table I. Each inhaler was tested under constant flow conditions of 30 and 60 L/min. For all experiments, an AIT was used as the induction port to mimic extrathoracic filtration. The aerosol exiting the AIT was interpreted as the *in vitro* lung dose. The lung dose was further divided into TB and alveolar doses using two distinct methods. In the first method, the aerosol exiting the AIT was supplied directly to the FBA, with the TB and alveolar doses collected on their respective, representative filters. In the second method, the aerosol exiting the AIT was characterized using a cascade impactor, with the results then being used as input to an *in silico* regional lung deposition model. For each experiment, regardless of the method employed, the inhaler was actuated into the apparatus five times and each experiment was repeated five times. Regional deposition estimates arising from the two experimental methods were then compared.

**Table 1** List of pMDI devices studied and select attributes

Inhaler <sup>1</sup>	API	Doses	Label Claim <sup>2</sup> (µg of API per actuation)	Formulation Type	Propellant	Excipients
Asmanex HFA [12]	Mometasone furoate	120	100	Suspension	HFA-227	Ethanol, oleic acid
QVAR [13]	Beclomethasone dipropionate	200	100	Solution	HFA-134a	Ethanol
Ventolin HFA [14]	Salbutamol sulfate	200	100	Suspension	HFA-134a	None

<sup>1</sup> Asmanex HFA was sourced in the United States while QVAR and Ventolin HFA were sourced in Canada. More information can be found in the applicable product monographs [12–14].

<sup>2</sup> For Asmanex HFA and Ventolin HFA, label claim is the ex-actuator delivered dose. For QVAR, the label claim is the ex-valve delivered dose.

## Filter-Based Regional Deposition Estimates

While the fundamental component of the filter-based approach when estimating regional deposition is the carefully-designed TB filter, the housing that holds this filter includes various additional functional design elements. Most notable are the use of an annular flow field and an integrated electrostatic neutralizer (Fig. 1). The housing inlet is machined to interface with the AIT outlet with an airtight seal and matching internal dimension to minimize particle losses. This 16 mm internal diameter section extends for 20 mm and then rapidly expands with a 60° draft angle to 75 mm. After expansion, the flow field is interrupted and abruptly changes to an annular shape with major and minor diameters of 75 and 45 mm, respectively. The top of the annular core (also called the flow disruptor plate) is 33 mm downstream from the onset of the rapid expansion; the axis of the core is colinear with the axis of the AIT outlet. Rapid expansion and interruption of the flow are used to force the laryngeal jet off the anterior wall of the AIT trachea and then distribute the energy into the bulk flow, providing a relatively uniform flow down the annular gap towards the TB filter. Without these flow alterations, the laryngeal jet would result in a localized section of high flow through the TB filter, causing the filter's face velocity and filtration to be higher than intended. As large particles penetrating the AIT may deposit at the flow disruption point, a collection dish is incorporated into the top of the annulus core. This dish has 5 mm tall walls and an internal diameter of 33 mm.

As the aerosol flows down the annular channel, it passes through a neutralizing section where alternating current corona discharge is used to generate bipolar ions. The outer electrode is an internally serrated ring of 0.003" (0.08 mm) thick 304 stainless steel located 33 mm downstream from the top of the annulus core. The tips of the serrations act as corona onset locations and are separated from the 'core electrode' by a distance of 17 mm; an electrode separation larger than the annular gap was used to keep the electrode tips out of the flow path. The outer electrode is axially centred on the core electrode, which is a smooth stainless-steel ring 15 mm long forming part of the annular core (diameter

of 45 mm). A potential difference of 5 kV is applied between the two electrodes which ionizes the air near the serrations of the outer electrode; the ions then travel across the annular gap towards the core electrode. If an ion encounters an oppositely charged aerosol particle along the way, it will be attracted to the particle and reduce its static charge. The exact charge state of aerosol leaving the neutralizing region has not been measured; however, filtration measurements have shown that the use of the neutralizer improves agreement between TB filter measurements and traditional methods of estimating regional deposition [11].

After leaving the neutralizing region, the aerosol encounters the TB filter. This filter has been carefully designed to have a filtration efficiency that mimics the average deposition efficiency of the TB region of the lungs [10], including both aerosol size and inhalation flow rate effects. The face area of this filter is an essential metric that dictates the annular radii. The filter is located 42 mm downstream of the outer electrode ring and 75 mm downstream of the top of the annular core. Two layers of highly specific stainless-steel mesh comprise the filter; the first layer uses 25 µm diameter wire woven with 500 wires per inch in each direction, while the second layer uses 30 µm wire and 400 wires per inch (SV-26/25tw, SV-34/30tw; ASADA MESH Co., Osaka, Japan). The stainless-steel mesh is spot welded between 1 mm thick stainless-steel rings to hold the mesh taught. As a result, the mesh filter elements are separated by 2 mm. After traversing the TB filter, the annular section extends for an additional 30 mm, then with a 45° draft angle the annulus core and outer walls constrict. The annulus cone ends when the diameter reaches 15 mm and the outer walls return to a straight pipe flow when the diameter reaches 18 mm. Finally, this straight pipe section extends for 29 mm to the outlet of the TB filter housing. A commercially available filter with a standard 22 mm ID connection (H8–6301; KEGO Corporation, London, Canada) installs on the outlet of the TB filter housing to collect the remaining aerosol. The total internal volume, or 'dead space', of the TB Filter housing is 488 mL, while the dead space from the inlet of the housing to the TB filter elements is 310 mL. A rendering of the TB Filter assembly can be seen in Fig. 1.

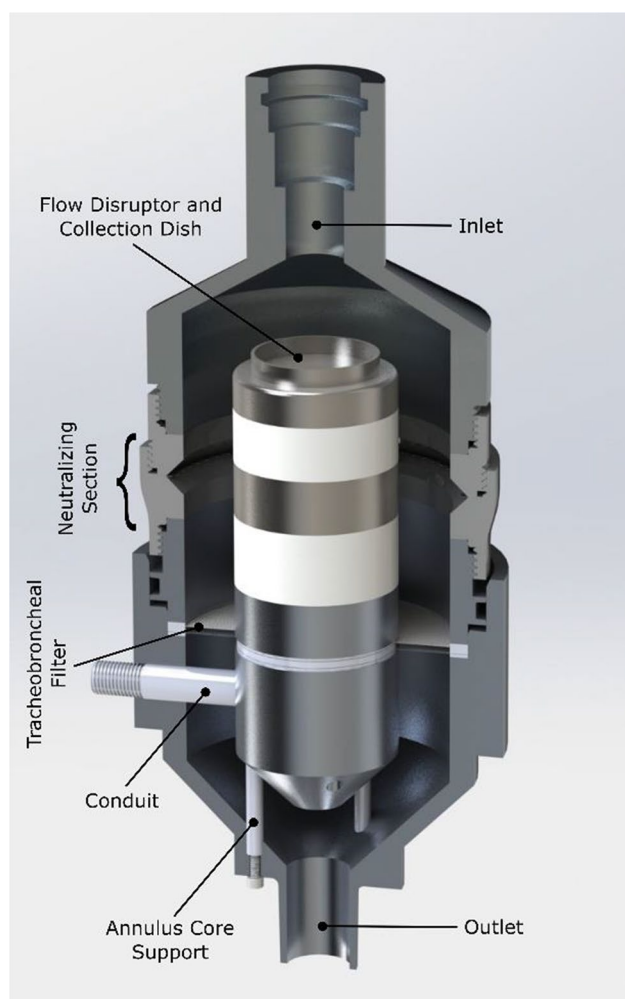


**Fig. 1** A partial section view of the TB Filter housing. External components have been sectioned to reveal the interior assembly and flow path to which the aerosol exiting the AIT is exposed.

The desired flow rate through the apparatus was generated by a vacuum pump (0523, Gast Manufacturing Inc., Benton Harbor, MI, USA), controlled using a needle valve, and monitored with a mass flow meter (4043, TSI Incorporated, Shoreview, MN USA). A schematic representation of this experimental configuration can be seen in Fig. 2.

### Cascade Impactor Based Regional Deposition Estimates

In the more traditional method of estimating regional deposition, the inhaler was actuated into the AIT, which was upstream of a Next Generation Impactor (NGI) including a pre-separator stage (MSP Corporation, Shoreview, MN, USA). A vacuum pump (Model KSV, General Signal, Canton, Massachusetts) generated the desired flow through the apparatus, which was set manually with a ball valve and

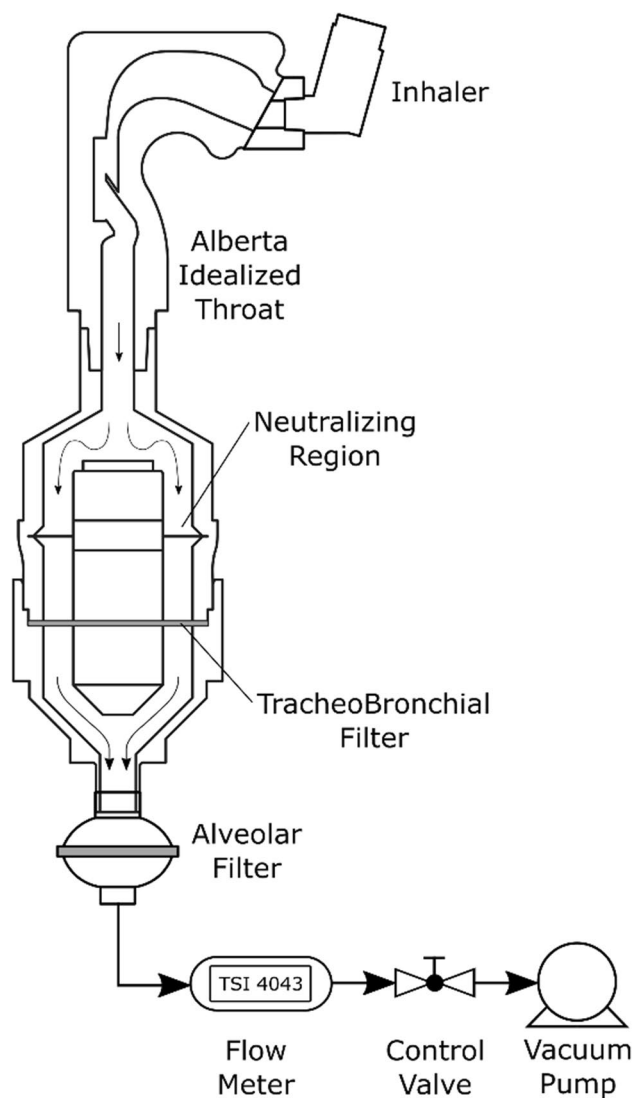


**Fig. 2** Schematic representation of the filter-based apparatus configured for constant flow.

monitored with a mass flow meter (4040, TSI Incorporated). A schematic representation of this experimental configuration can be seen in Fig. 3.

Aerodynamic particle size distributions determined using the NGI were used as input to the *in silico* regional deposition model described by Javaheri *et al.* [15]. Since the AIT was already used to remove the extrathoracic fraction, extrathoracic deposition was not modeled. The model divides the breath into 1000 bolus fractions and propagates each one sequentially through a 1D symmetrical branching lung model with dimensions given by [16]. The aerosol classified by the NGI is evenly distributed between all bolus fractions and thus not all particles will reach the final generation of the model lung. Deposition equations for sedimentation [17, 18], diffusion [19], and impaction [20] are used to estimate deposition in each generation of the lung

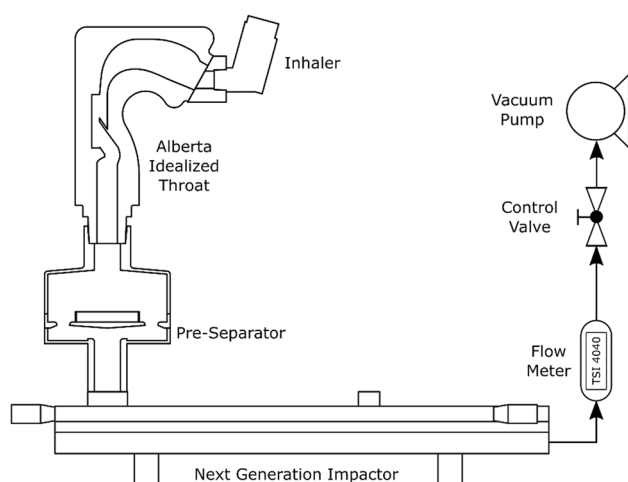


**Fig. 3** Schematic representation of the NGI apparatus configured for constant flow.

under inhalation, breath hold, and exhalation. In this study the inhaled volume was 2.7 L, the inhalation time was set to 5.4 s or 2.7 s corresponding to 30 and 60 L/min inhalation flow rate, a breath hold of 10.0 s was used and exhalation time was 7.0 s. The model permits aerosol that evades deposition in the lung to be exhaled, which is important in predicting lung deposition for some nebulized aerosols inhaled under tidal breathing [21]. However, for single breath inhalers it is expected that most aerosol will deposit due to gravitational settling during breath holding [22]. Indeed, the exhaled dose calculated for the conditions used here is less than 10% of the lung dose, so, to draw a closer comparison to the filter-based apparatus, we use only the TB estimate from this model, while the alveolar dose is considered to be the lung dose less the TB estimate.

## Experimental Procedure

Ambient conditions were recorded on each day of experimentation; ambient air temperature and relative humidity were recorded from a digital thermometer/hygrometer (TH-1, Amprobe, Everett, WA, USA), and atmospheric pressure was recorded from the mass flow meters while they were open to the atmosphere under zero flow.

Collection surfaces of the AIT, NGI, and pre-separator were coated with silicone release spray (Molycote 316; Dow Corning, Midland, MI, USA) to reduce particle bounce and re-entrainment. To allow the propellant and solvents in the spray to evaporate, 15 min was allowed to elapse after spraying before the instruments were assembled. To ensure full collection of any particles impacting at the flow disruptor plate, ~2 mL of the assay solvent was added to the collection dish; a disc of stainless-steel mesh was fitted into the bottom of the collection dish to promote wetting of the surfaces

while using less solvent to reduce the chance of solvent splashing over the collection dish walls (which was observed to occur occasionally during preliminary experiments). No surface preparation was required for the TB Filter elements or the commercial final filter.

A 3D-printed adapter, unique to each inhaler tested, was affixed to the AIT inlet. These adapters closely matched the mouthpiece geometry, ensuring a snug, airtight fit and consistent positioning of the inhaler relative to the AIT inlet. The adapters used in this study hold the inhaler in the ‘transverse’ orientation to the AIT, i.e., the axis of the mouthpiece and the aerosol plume is horizontal despite the axis of the oral cavity of the AIT being angled upwards at 29° (see Fig. 2 or Fig. 3). In this orientation, the aerosol plume is directed towards the surface of the tongue, which can cause increased extrathoracic deposition depending on the pMDI properties [23]. This orientation is expected to be more representative of *in vivo* usage of inhalers [23].

With the collection surfaces adequately prepared and the appropriate adapter affixed to the AIT inlet, the equipment was assembled into the configuration being used (NGI or FBA). The vacuum pump was turned on and throttled to the appropriate volumetric flow rate; at this point the apparatus was ready for the inhaler to be actuated into it. Inhalers were primed following the leaflet directions before use for the first time; Ventolin HFA and Asmanex HFA were shaken well before every actuation, whereas QVAR was not, as per leaflet instructions. The vacuum pump remained on for the duration of the experiment; for runs with the TB Filter apparatus, the neutralizer was switched on just prior to actuating the inhaler and switched off approximately two seconds afterwards. The inhaler was removed from the AIT inlet and approximately ten seconds was allowed to elapse before the next actuation was performed.

After five actuations of the inhaler, the vacuum pump was switched off and API was recovered from collection surfaces by rinsing with HPLC grade methanol (Asmanex HFA and QVAR) or a 1:1 v/v mixture of HPLC grade methanol and deionized micron filtered water (Ventolin HFA). The AIT and alveolar filters were extracted with 25 mL of solvent divided into three washings but collected into a single 25 mL sample. The NGI and pre-separator impactor plates and the flow disruptor plate were washed with 5 mL of solvent, while the TB Filter was washed with 10 mL. When testing with QVAR, only 6 mL was used to extract API from the TB Filter to increase the sample concentration since TB deposition with QVAR is low. Ultraviolet light absorbance was used to quantify the mass of API in each sample; absorbance was measured using a spectrophotometer (Cary 8454, Agilent, Santa Clara, CA, USA) and concentration was quantified relative to absorbance measured in a series of dilutions of a prepared stock solution. Absorbance was measured at 226,

240, and 248 nm for salbutamol sulfate (Ventolin HFA), beclomethasone dipropionate (QVAR), and mometasone furoate (Asmanex HFA), respectively. Blank samples were made by preparing and washing the collection surfaces following the normal experimental procedure but without actuating the inhaler into the apparatus; absorbance was measured relative to these blank samples to eliminate interference of external compounds potentially absorbing near the API peak. Five replicate measurements were performed for each combination of inhaler, flow rate, and experimental configuration. Statistical comparisons were performed in Microsoft Excel 2019 (Microsoft, Redmond, WA, USA) using two-tailed, unpaired students t-tests.

## Results

Experiments were performed at ambient conditions (temperature, pressure, relative humidity) ranging from 21.0 to 24.7°C, 91.6 to 94.2 kPa, and 8.0 to 29.3% RH. Total recovered dose was independent of the experimental configuration ( $p > 0.05$ ) and was  $110.5 \pm 4.1\%$  of the label claim for Ventolin HFA,  $96.7 \pm 4.3\%$  of the label claim for Asmanex HFA, and  $65.5 \pm 5.5\%$  of the label claim for QVAR. For Asmanex HFA and QVAR, no API was detected on either the pre-separator or the flow disruptor plate. For Ventolin HFA, API detected on the pre-separator was independent of flowrate ( $p > 0.05$ ) and was only  $3.3 \pm 1.9 \mu\text{g}$  (less than 1% of recovered API). API was detected on the flow disruptor plate for only two runs with Ventolin at 60 L/min (13.3 and 2.8  $\mu\text{g}$ ) when testing with the TB Filter apparatus. Since API on the pre-separator and flow disruptor plate was generally zero or negligible, it was added to the mass recovered in the AIT, consistent with our previous study [11], and we have termed this aggregate upper respiratory tract (URT) deposition.

The aerodynamic particle size distribution data from the cascade impactor runs is given in Fig. 4 and Fig. 5. The regional deposition estimates from this data are shown in Table II alongside the regional deposition estimates given directly by the regional deposition filter apparatus. Graphical comparison of the regional deposition estimates given by the two different experimental configurations is shown in Fig. 6.

## Discussion

The FBA was developed with the intention of alleviating the burden associated with compendial testing methods when estimating regional deposition. The resource burden is vastly reduced in the laboratory by reducing the number of collection surfaces to assay. There are only four

collections surfaces to assay when using the FBA (AIT, flow disruptor plate, TB Filter, alveolar filter) but 10 collections surfaces when using the NGI (AIT, pre-separator, 8 NGI stages). The resource burden associated with interpreting the results using the FBA is nearly completely eliminated because there is no post processing required to arrive at regional deposition estimates since they are measured directly. The lung dose is well quantified by adopting the AIT as the induction port; if the TB Filter removes the appropriate dose from the flow, then both the TB and alveolar fractions will be accurately estimated.

The comparison of regional deposition estimates given by the two methods in Fig. 6 demonstrates that the filter-based method can provide reasonable estimates that account for differences due both to particle size and to inhalation flow rate. The particle size dependence is not explicitly shown in Fig. 6; however, the inhalers have been grouped from smallest to largest MMAD along the x-axis to demonstrate the effect of particle size. From this manner of grouping, it appears that the TB Filter somewhat over-predicts TB deposition relative to the regional deposition model for coarser aerosols. This result is not unexpected as the filtration curves for the TB Filter given by [10] were given only for particle sizes up to 3.3  $\mu\text{m}$ , and the filter curves appear to cross above the deposition model curve around this point. For Asmanex (where the difference between estimates is greatest), there is significant mass reaching the *in vitro* lungs in particles larger than 3.3  $\mu\text{m}$ , which will be collected in greater proportions than the *in silico* regional deposition model predicts. We consider this difference to be acceptable for the reasons that follow. First, the *in silico* regional deposition model is used here only as a guide, since the *in silico* result will depend on which regional deposition model (of which there are many) is used, and *in vivo* regional deposition will vary considerably from person to person. Furthermore, statistically significant differences in regional deposition estimates here are largely the result of the high repeatability of each method (with commensurately small standard deviations), and it is unlikely these differences would translate to clinically significant differences.

Exploratory experiments were conducted to investigate the effect of electrostatic charge on the filtration of the TB Filter and the necessity of using the neutralizer. While we have not explicitly measured the charge state of the pMDI aerosols used here before and after neutralization by our custom ion generator, we conducted limited measurements with and without powering the neutralizer to investigate its effectiveness. These measurements were performed for the QVAR and Ventolin HFA inhalers, both of which were also studied by Leung *et al.* [24] who measured the bipolar charge distribution of aerosols emitted by the pMDIs using a Bipolar Charge Analyzer (BOLAR).

**Fig. 4** Mass of API detected on each stage of the NGI when operated at 30 L/min; absence of a data bar indicates no API detected. Diameter values listed are the geometric centres for each stage. Error bars represent the standard deviation of  $n=5$  repeat measurements. Log-normal distribution parameters for each inhaler, listed as MMAD  $\pm$  GSD, are: Asmanex HFA  $3.26 \mu\text{m} \pm 1.60$ , Ventolin HFA  $2.03 \mu\text{m} \pm 1.61$ , QVAR  $1.03 \mu\text{m} \pm 1.80$ .

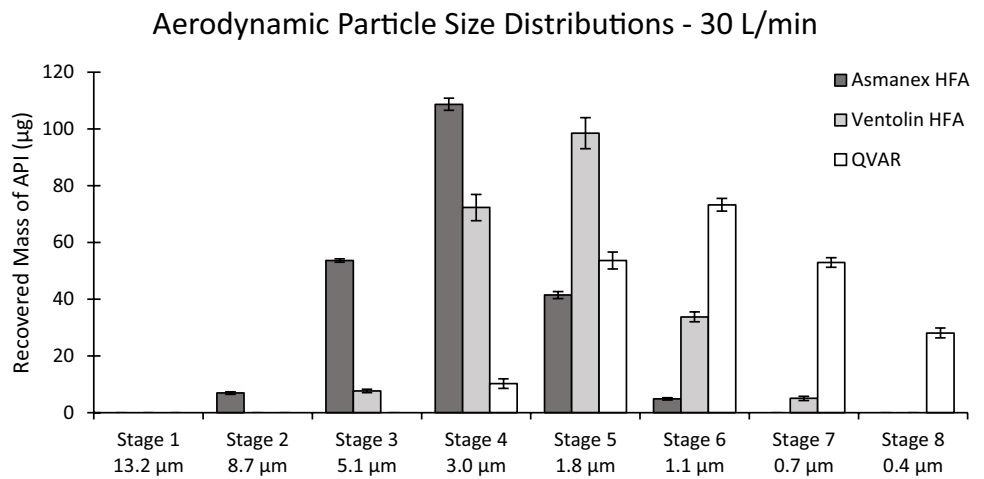


**Fig. 5** Mass of API detected on each stage of the NGI when operated at 60 L/min; absence of a data bar indicates no API detected. Diameter values listed are the geometric centres for each stage. Error bars represent the standard deviation of  $n=5$  repeat measurements. Log-normal distribution parameters for each inhaler, listed as MMAD  $\pm$  GSD, are: Asmanex HFA  $3.22 \mu\text{m} \pm 1.61$ , Ventolin HFA  $2.07 \mu\text{m} \pm 1.64$ , QVAR  $0.85 \mu\text{m} \pm 1.87$ .

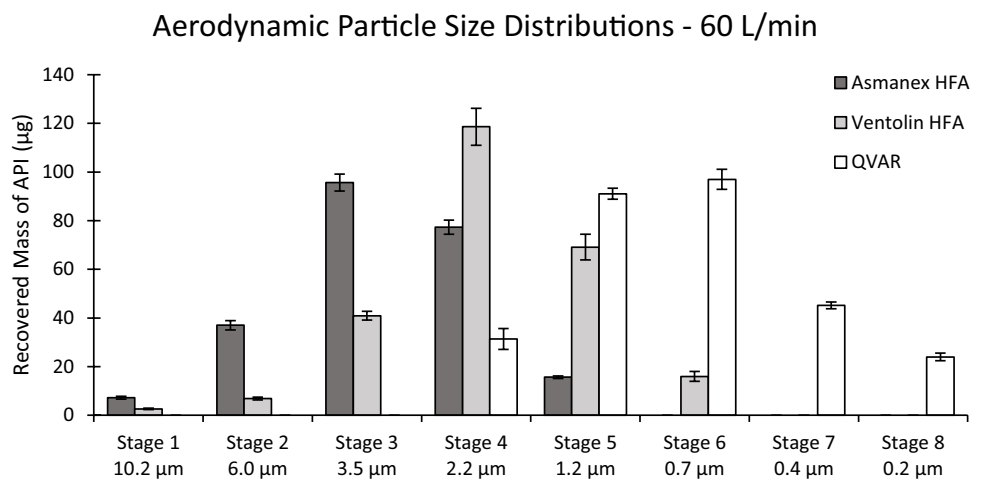
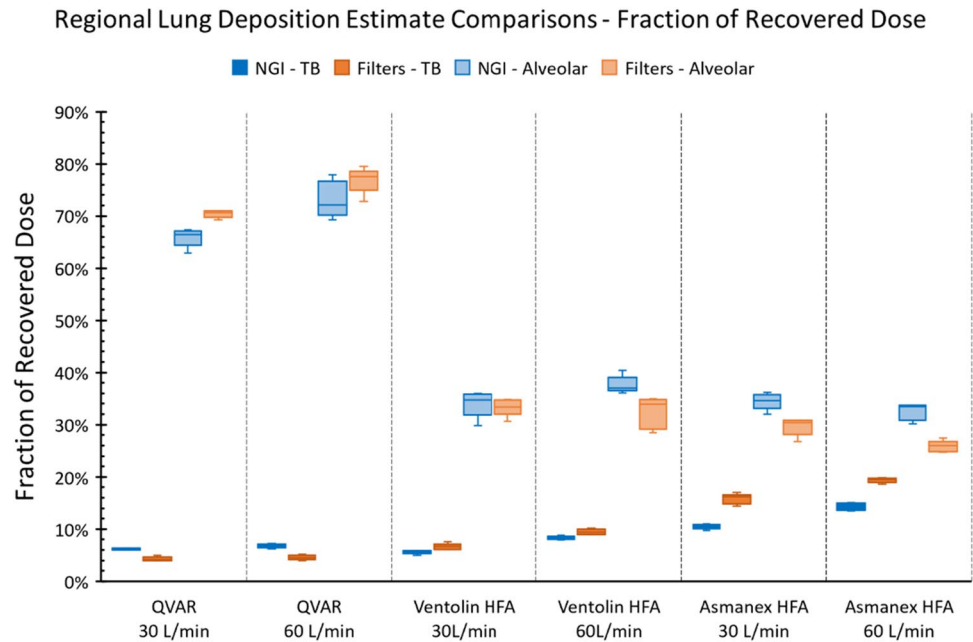


**Table II** Comparison of regional deposition estimates from the two experimental methods; modeled after cascade impactor measurements (NGI+RegDep) or measured directly using the filter-based apparatus (Filters). Results are given as mass of API, listed as average  $\pm$  standard deviation for  $n=5$  runs. Asterisk between values indicates statistically significant difference using a Student’s t-test ( $p < 0.05$ )

		QVAR		Ventolin HFA		Asmanex HFA	
		NGI+RegDep	Filters	NGI+RegDep	Filters	NGI+RegDep	Filters
30 L/min	URT (μg)	84.9 $\pm$ 9.2	78.7 $\pm$ 1.7	331.6 $\pm$ 23.7	335.0 $\pm$ 23.5	263.3 $\pm$ 17.0	261.0 $\pm$ 19.8
	TB (μg)	18.6 $\pm$ 0.9 *	13.3 $\pm$ 1.4	30.7 $\pm$ 1.6 *	37.0 $\pm$ 2.4	50.5 $\pm$ 0.8 *	75.7 $\pm$ 3.9
	Alveolar (μg)	199.5 $\pm$ 8.1 *	218.9 $\pm$ 5.6	186.6 $\pm$ 9.7	185.7 $\pm$ 8.8	165.1 $\pm$ 2.7 *	142.0 $\pm$ 5.6
	Total (μg)	303.0 $\pm$ 16.4	310.9 $\pm$ 7.4	548.9 $\pm$ 19.2	557.7 $\pm$ 27.8	478.9 $\pm$ 15.0	478.7 $\pm$ 19.8
60 L/min	URT (μg)	72.9 $\pm$ 15.2	62.5 $\pm$ 12.7	298.9 $\pm$ 9.8	320.6 $\pm$ 17.0	264.8 $\pm$ 22.3	262.0 $\pm$ 11.7
	TB (μg)	24.6 $\pm$ 0.7 *	15.2 $\pm$ 0.8	45.8 $\pm$ 2.5 *	52.0 $\pm$ 2.7	71.2 $\pm$ 2.9 *	92.7 $\pm$ 3.0
	Alveolar (μg)	263.9 $\pm$ 4.5	256.9 $\pm$ 8.4	208.3 $\pm$ 12.1 *	178.4 $\pm$ 15.4	161.7 $\pm$ 5.5 *	123.8 $\pm$ 6.1
	Total (μg)	361.4 $\pm$ 16.0	334.7 $\pm$ 20.4	553.0 $\pm$ 15.4	550.9 $\pm$ 15.2	497.7 $\pm$ 25.7	478.5 $\pm$ 16.7

**Fig. 6** Comparison of regional deposition estimates for each inhaler and flow rate studied. For the ‘NGI’ series, the regional deposition estimates are the results of using cascade impactor data as input to the regional deposition model given by Javaheri *et al.*, while for the ‘Filter’ series the regional deposition estimates are measured directly.



We have previously discussed electrostatic effects in detail [11] and do not expect the charge levels associated with pharmaceutical aerosols to significantly affect *in vivo* deposition in the TB region. However, electrostatic charge on the aerosol can significantly affect the filtration efficiency of the stainless-steel TB Filters, where image charges will readily be induced due to their conductive nature. The pore sizes of the TB Filters are 25 and 30  $\mu\text{m}$ , whereas the diameter of the most distal generation of the TB region of the lung is expected to have a diameter around  $20\times$  larger [9]. Electrostatic attractive forces are inversely proportional to the squared separation distance, so the electrostatic attractive force in the TB Filter could be  $400\times$  higher than in the most distal generation of the TB region, and even higher in more proximal generations.

In the present experiments, when the neutralizer was not powered, deposition on the TB filter increased by 82% and 30% relative to experiments where the neutralizer was active for QVAR and Ventolin HFA, respectively. These results are aligned with the charge distributions measured by Leung *et al.* [24], who found that QVAR and Ventolin produced aerosols with very different charge characteristics. Ventolin HFA produced aerosol with relatively low charge-to-mass ratios ( $\sim 25$  pC/ $\mu\text{g}$ ) and no API was detected in the smallest size bin of the BOLAR ( $d_p < 0.95$   $\mu\text{m}$ ), whereas the smallest bin collected the most mass when testing the QVAR, and the charge-to-mass ratio magnitude associated with these particles was  $> 200$  pC/ $\mu\text{g}$ . The highly charged, small particles associated with the QVAR are likely the most susceptible to electrostatic effects due to their high physical mobility. Further, more extremely charged particles could drive the deposition enhancement while mildly

charged particles are less affected. The increase in deposition on the TB Filter when the neutralizer is not used is in relative agreement with the magnitude of previously measured charge profiles for these inhalers.

The two experimental configurations provide similar results for upper respiratory deposition, as the AIT was used as an induction port in both experiments. For this study, the total recovered dose from each inhaler was used to compare the recovery efficiency of the filter-based method to the established, cascade impactor method. No significant difference in recovered dose was seen between the two methods, indicating the particle losses within the NGI and the TB Filter housing are similar. While this was the primary comparison, it was also expected that total recovered dose would lie between 75 and 125% of the label claim as required by [2]. The recovered dose we found for QVAR was not within this range, but this is largely explained by the fact that the label claim is the ex-valve dose. The product monograph [13] states that each actuation delivers 80  $\mu\text{g}$  from the actuator. Using 80  $\mu\text{g}$  as the ‘label claim’ changes the recovered dose here to  $81.9 \pm 6.9\%$ . Furthermore, QVAR was the only inhaler we studied where total recovery depended on the flow rate. When testing at 30 L/min, total recovery was  $76.7 \pm 3.3\%$  of the ex-actuator claim, whereas total recovery was  $87.0 \pm 5.7\%$  of the ex-actuator claim when testing at 60 L/min ( $p = 0.00018$ ). While the dose remaining in the actuator was not quantified in this study, we surmise that there is increased deposition in the actuator at lower flow rates, possibly due to better entrainment of the aerosol plume at higher flow rates. In terms of mass of API, we recovered  $65.5 \pm 5.5$   $\mu\text{g}$  per actuation ( $61.4 \pm 2.7$   $\mu\text{g}$  and  $69.6 \pm 4.5$   $\mu\text{g}$  at 30 and 60 L/min, respectively), a result



that compares reasonably to those reported by [25] who recovered  $74.3 \pm 13.9$   $\mu\text{g}$  per actuation for QVAR. Finally, we measured the recovered API when actuating the inhaler directly into a filter through which 60 L/min was being generated by a downstream vacuum pump ( $n = 3$  replicate measurements). In these confirmatory tests we recovered  $71.1 \pm 4.3$   $\mu\text{g}$  of API per actuation ( $88.9 \pm 5.3\%$  of ex-actuator claim), indicating that the mass of API recovered in the regional deposition measurements was typical for this particular inhaler.

The differences in regional deposition due to flow rate seen for each inhaler require considering more than just the particle dynamics of an inhaled aerosol. If particle dynamics alone dictated the regional deposition estimate, one might expect the TB fraction to increase with flow rate (due to increased deposition due to impaction) and thus cause the alveolar fraction to decrease. However, for QVAR the fraction of delivered dose reaching the alveolar region increases with flow rate while the TB dose remains relatively unchanged. The TB Filtration curve is relatively flat for the small particle sizes associated with the QVAR aerosol plume, a result that agrees with the small changes to TB Filtration. The increase in alveolar dose is due to reduced extrathoracic deposition, which may result from improved entrainment of the aerosol plume. Most important is that this trend is captured consistently by both experimental methods. Liu *et al.* [26] measured the droplet velocities and impaction forces of the aerosol plumes emitted from various pMDIs, including QVAR and Ventolin HFA. They showed that droplet velocities and plume impaction forces were positively correlated and significantly lower for the QVAR device than for the Ventolin HFA. While the droplet mass at impaction could not be measured, these measurements provide a good estimate of plume momentum, as was used by Ruzycki *et al.* [23] to describe the dependence of extrathoracic deposition on inhaler orientation observed for the Ventolin Evohaler (equivalent to Ventolin HFA) but not for the QVAR device. The moderate difference in inhalation flow rate used in this study does not affect extrathoracic deposition for the relatively high momentum plumes of Ventolin HFA and Asmanex HFA. Combined with the larger particle sizes associated with these inhalers, the regional lung deposition estimates follow the expected trend of increasing TB deposition with flow rate. Overall, the expected change in TB deposition due to flow rate is well captured by the filter-based apparatus as compared to the *in silico* deposition model used here. It should be noted that, due to the use of a constant flow rate in this study, the effect on deposition due to flow rate identified here is void of any effects relating either to the shape of inhalation profile performed by the patient or to (in)coordination of inhaling and actuating the pMDI. We

chose to eliminate these effects in the present work both because doing so enabled straightforward comparison of regional deposition estimates obtained at different flow rates and because the FBA has previously been validated for use with time varying inhalation profiles [11]; future work is planned to investigate the effects of breath/actuation timing on regional deposition estimates arising from the FBA.

## Conclusions

A novel, filter-based apparatus downstream of an Alberta Idealized Throat extrathoracic airway was used to fractionate the *in vitro* lung dose into TB and alveolar regional deposition estimates for various commercially available pMDI devices. The same devices were tested in a more conventional manner using an NGI to classify the *in vitro* lung dose, with the results then used as input to an *in silico* regional deposition model. The inhalers used here provide a wide variety of aerosol sizes (MMAD ranging from 0.9 to 3.3  $\mu\text{m}$ ) and were each tested at 30 and 60 L/min. The regional deposition estimates from each method were in good agreement, indicating the filter-based approach can capture effects due to particle size and inhalation flow rate while requiring far less time and fewer resources to perform. This approach therefore has the potential both to expedite research and development of novel inhalation therapies exploiting targeted delivery to a distinct region of the lungs, and to expedite comparisons of equivalence between innovator products and second-entry generics.

**Acknowledgements** The authors thank ASADA Mesh Company for supplying materials to construct the filter elements.

**Funding** This research was financially supported by Proveris Scientific Corporation.

## Declarations

**Conflict of Interest** Patents have been filed on the technology described in this work, which may financially benefit the authors.

## References

1. European Directorate for the Quality of Medicines & HealthCare. European Pharmacopoeia 7.0 Vol 1 Section 2.9.18 Preparations for inhalations: Aerodynamic assessment of fine particles. Strasbourg: Ph.Eur; 2010
2. United States Pharmacopeia. USP 44(5) General Chapter <601> Inhalation and Nasal Drug Products - Aerosols, Sprays, and Powders - Performance Quality Tests. Rockville: USP-NF; 2019.
3. Newman SP. Fine Particle Fraction: The Good and the Bad. *J Aerosol Med Pulm Drug Deliv.* 2022;35:2–10.
4. Mitchell JP, Nagel MW (2022) Merging pharmacopeial and clinically relevant oral inhaler testing streams: All or nothing or is there a middle way? *Inhalation* 22–30.

5. Ruzycki CA, Murphy B, Nathoo H, Finlay WH, Martin AR (2020) Combined in Vitro-in Silico Approach to Predict Deposition and Pharmacokinetics of Budesonide Dry Powder Inhalers. *Pharmaceutical Research: An Official Journal of the American Association of Pharmaceutical Scientists*. <https://doi.org/10.1007/s11095-020-02924-7>.
6. Copley M. Improving inhaled product testing: Methods for Obtaining Better In vitro-In vivo Relationships. *Pharm Technol*. 2013;37:42–7.
7. Mitchell JP, Nagel MW, Avvakoumova V, MacKay H, Ali R. The Abbreviated Impactor Measurement (AIM) Concept: Part 1-Influence of Particle Bounce and Re-Entrainment-Evaluation with a “Dry” Pressurized Metered Dose Inhaler (pMDI)-Based Formulation. *AAPS PharmSciTech*. 2009;10:243–51.
8. Mitchell JP, Suggett J, Nagel M. Clinically Relevant In Vitro Testing of Orally Inhaled Products-Bridging the Gap Between the Lab and the Patient. *AAPS PharmSciTech*. 2016;17:787–804.
9. Finlay WH, Gehmlich MG. Inertial sizing of aerosol inhaled from two dry powder inhalers with realistic breath patterns versus constant flow rates. *Int J Pharm*. 2000;210:83–95.
10. Tavernini S, Kiaee M, Farina DJ, Martin AR, Finlay WH. Development of a filter that mimics tracheobronchial deposition of respirable aerosols in humans. *Aerosol Sci Technol*. 2019;53:802–16.
11. Tavernini S, Farina DJ, Martin AR, Finlay WH. Using Filters to Estimate Regional Lung Deposition with Dry Powder Inhalers. *Pharm Res*. 2021;38:1601–13.
12. Merck & Co. Inc., ASMANEX® HFA (Mometasone Furoate) Inhalation Aerosol, for Oral Inhalation Use [product monograph]. 2018 [cited 2022 Oct 12]. Available from: [https://www.accessdata.fda.gov/drugsatfda\\_docs/label/2018/205641s007s0081bl.pdf](https://www.accessdata.fda.gov/drugsatfda_docs/label/2018/205641s007s0081bl.pdf).
13. Bausch Health Canada Inc., QVAR Beclomethasone Dipropionate Inhalation Aerosol [product monograph]. 2020 [cited 2022 Oct 12]. Available from: [https://pdf.hres.ca/dpd\\_pm/00059601.PDF](https://pdf.hres.ca/dpd_pm/00059601.PDF).
14. GlaxoSmithKline Inc., VENTOLIN HFA Salbutamol Pressurised Inhalation Suspension [product monograph]. 2021 [cited 2022 Oct 12]. Available from: [https://pdf.hres.ca/dpd\\_pm/00060404.PDF](https://pdf.hres.ca/dpd_pm/00060404.PDF).
15. Javaheri E, Shemirani FM, Pichelin M, Katz IM, Caillibotte G, Vehring R, Finlay WH. Deposition modeling of hygroscopic saline aerosols in the human respiratory tract: Comparison between air and helium–oxygen as carrier gases. *J Aerosol Sci*. 2013;64:81–93.
16. Finlay WH, Lange CF, King M, Speert DP. Lung Delivery of Aerosolized Dextran. *Am J Respir Crit Care Med*. 2000;161:91–7.
17. Heyder J (1975) Gravitational deposition of aerosol particles within a system of randomly oriented tubes. 6:133–137.
18. Heyder J, Gebhart J. Gravitational deposition of particles from laminar aerosol flow through inclined circular tubes. *J Aerosol Sci*. 1977;8:289–95.
19. Ingham DB (1975) Diffusion of Aerosols from a Stream Flowing through a Cylindrical Tube. *J Aerosol Sci* 125–132.
20. Chan TL, Lippmann M. Experimental measurements and empirical modelling of the regional deposition of inhaled particles in humans. *Am Ind Hyg Assoc J*. 1980;41:399–409.
21. Yang MY, Ruzycki C, Verschuer J, Katsifis A, Eberl S, Wong K, Golshahi L, Brannan JD, Finlay WH, Chan H-K. Examining the ability of empirical correlations to predict subject specific in vivo extrathoracic aerosol deposition during tidal breathing. *Aerosol Sci Technol*. 2017;51:363–76.
22. Martin AR, Moore CP, Finlay WH. Models of deposition, pharmacokinetics, and intersubject variability in respiratory drug delivery. *Expert Opin Drug Deliv*. 2018;15:1175–88.
23. Ruzycki CA, Martin AR, Finlay WH. An Exploration of Factors Affecting in Vitro Deposition of Pharmaceutical Aerosols in the Alberta Idealized Throat. *J Aerosol Med Pulm Drug Deliv*. 2019;32:405–17.
24. Leung SSY, Chiow ACM, Ukkonen A, Chan HK. Applicability of Bipolar Charge Analyzer (BOLAR) in Characterizing the Bipolar Electrostatic Charge Profile of Commercial Metered Dose Inhalers (MDIs). *Pharm Res*. 2016;33:283–91.
25. Kwok PCL, Glover W, Chan HK. Electrostatic charge characteristics of aerosols produced from metered dose inhalers. *J Pharm Sci*. 2005;94:2789–99.
26. Liu X, Doub WH, Guo C. Evaluation of metered dose inhaler spray velocities using Phase Doppler Anemometry (PDA). *Int J Pharm*. 2012;423:235–9.

**Publisher's Note** Springer Nature remains neutral with regard to jurisdictional claims in published maps and institutional affiliations.

Springer Nature or its licensor (e.g. a society or other partner) holds exclusive rights to this article under a publishing agreement with the author(s) or other rightsholder(s); author self-archiving of the accepted manuscript version of this article is solely governed by the terms of such publishing agreement and applicable law.